Geophysical Research Letters

RESEARCH LETTER
10.1029/2021GL095336

Mixing Enhancement Mechanisms in Aquifers Affected by Hydropeaking: Insights From Flow-Through Laboratory Experiments

F. Ziliotto[1], M. Basilio Hazas[1], M. Rolle[2], and G. Chiogna[1]

[1]Chair of Hydrology and River Basin Management, Technical University of Munich, Munich, Germany, [2]Department of Environmental Engineering, Technical University of Denmark, Lyngby, Denmark

Key Points:

- Flow-through laboratory experiments demonstrate hydropeaking-enhanced plume mixing, controlled by local dispersion and spreading
- High-resolution spatio-temporal analysis of solute distribution to quantify spreading and mixing in highly transient flow fields
- Hydropeaking affects plume arrival times and induces fluctuating, multi-modal breakthrough curves

Supporting Information:

Supporting Information may be found in the online version of this article.

Correspondence to:

G. Chiogna and M. Rolle,
gabriele.chiogna@tum.de;
masro@env.dtu.dk

Citation:

Ziliotto, F., Basilio Hazas, M., Rolle, M., & Chiogna, G. (2021). Mixing enhancement mechanisms in aquifers affected by hydropeaking: Insights from flow-through laboratory experiments. *Geophysical Research Letters*, *48*, e2021GL095336. https://doi.org/10.1029/2021GL095336

Received 22 JUL 2021
Accepted 13 OCT 2021

Abstract This study presents high-resolution flow-through experiments investigating transport processes in a laboratory setup mimicking an aquifer affected by hydropeaking (i.e., abrupt fluctuations in the river stage by the release or storage of water in reservoirs). Highly transient flow conditions were experimentally generated by sudden changes of the water level in two rivers in hydraulic contact with an unconfined aquifer. High-resolution image analysis and depth-resolved, high-frequency sampling at the outlet allowed monitoring of the spatio-temporal evolution and the breakthrough of a dye tracer plume in the porous medium. The plume spreading and mixing were quantified by moment analysis and entropy-based metrics of the scalar field. We show that hydropeaking strongly enhances spreading and mixing in the subsurface (up to 249.5% and 41.8% in these experiments) and demonstrate the relevance of considering highly transient flow regimes to properly capture transport and mixing-controlled biogeochemical reactions at the surface water - groundwater interface.

Plain Language Summary Mixing processes in porous materials, such as aquifers, are generally slow and inefficient. In this study, we performed laboratory experiments to demonstrate that if the fluid velocity rapidly changes in space and time, mixing can be enhanced. The experimental setup reproduces conditions that are relevant for understanding river-aquifer interactions and in particular the situation in which the water level in rivers rapidly changes due to the operation of hydropower plants. Our study helps understand transport in these systems and has important implications on the behavior of contaminants and nutrients at the interface between surface water and groundwater.

1. Introduction

The mixing of fluids is relevant in many fields of science and engineering over a large range of time and length scales (Aref et al., 2017; Kitanidis, 1994; Ottino, 1990; Rolle & Le Borgne, 2019; Valocchi et al., 2019). Mixing is strongly associated with stretching and deformation in the flow field (Ottino, 1990) and with the combined action of advection and diffusion mechanisms (Turuban et al., 2019). In geophysical flows, mixing affects biogeochemical cycles, mineral precipitation/dissolution, carbon sequestration, oil recovery, and surface water and groundwater contamination and remediation (e.g., Cardenas et al., 2004; Chiogna et al., 2012; Cil et al., 2017; Wallace et al., 2020; Zhang et al., 2010).

In porous media, mixing is often slow and incomplete thus constituting the overall rate-limiting step of many biogeochemical processes (Sole-Mari et al., 2020; Valocchi et al., 2019; Wright et al., 2017). Therefore, identifying the mechanisms that can enhance mixing is of great importance, in particular at the millimeter to meter scale where mixing-controlled reactions often occur in a very thin (bio)reactive fringe (Bauer et al., 2009; Hester et al., 2017; Rolle et al., 2013). At the pore scale, fingering structures (de Anna et al., 2014; Jiménez-Martínez et al., 2016) and chaotic advection (Heyman et al., 2020; Lester et al., 2013, 2016; Souzy et al., 2020; Turuban et al., 2019) enhance mixing and exert a key control on dispersion and reaction rates. At the Darcy scale, anisotropic (Chiogna et al., 2015; Ye et al., 2015a, 2018) and heterogeneous flow fields (e.g., de Barros et al., 2012; Dentz et al., 2016) enhance plume dilution and reactive mixing. Variability in the hydraulic conductivity fields (Rolle et al., 2009; Werth et al., 2006; Ye et al., 2015c), topographic features (Bandopadhyay et al., 2018), and transient conditions (e.g., de Dreuzy et al., 2012; Kahler & Kabala, 2016; Piscopo et al., 2013; Sposito, 2006; Trefry et al., 2019) lead to spatially variable flow fields.

Transient flow fields are important both in natural and engineered subsurface systems (Piscopo et al., 2013; Singh et al., 2020). For instance, in coastal aquifers, the combined effect of tides and regional groundwater flow impacts mixing and reactive processes (Geng et al., 2020; Trefry et al., 2019; Wu, Lester, et al., 2020), influencing salinity distributions and biogeochemical processes. Among engineered applications, in the field of groundwater remediation, transient flow fields have been proposed to enhance reactant delivery and contaminant degradation (Bagtzoglou & Oates, 2007; Neupauer et al., 2014; Reising et al., 2018; Rodríguez-Escales et al., 2017; Zhang et al., 2009). Transient flow fields and their effect on spreading, including the theoretical derivation of an effective dispersion tensor have been also analyzed in previous studies (Bolster et al., 2009; de Dreuzy et al., 2012; Dentz & Carrera, 2003, 2005). These studies focused on heterogeneous porous media and on the evolution of spreading toward an asymptotic behavior. Effective and macrodispersion coefficients were commonly expressed as a function of the heterogeneous properties of the porous medium. Our focus here is on mixing occurring in aquifer systems affected by hydropeaking in hydraulically connected rivers, where sudden fluctuations in river stage at the sub-daily scale are caused by the release or storage of water in artificial reservoirs. This hydrological regime leads to sharp and frequent fluctuations in the groundwater velocity field, altering the flux and solute exchange between the river and the aquifer and, in combination with the geomorphic features of the river, it plays an important role in physical, geochemical, thermal and biological processes in the hyporheic zone (Cardenas et al., 2004; Ferencz et al., 2019; Hester et al., 2013; Sawyer, Bayani Cardenas, et al., 2009; Schmadel et al., 2016; Shuai et al., 2019; Song et al., 2018; Wu et al., 2018, Wu, Gomez-Velez, et al., 2020). Hydropeaking affects sediment and solute transport in the river (Béjar et al., 2018; Pulg et al., 2016), as well as, biogeochemical cycles (Maavara et al., 2020) and riverine ecosystems (Gillespie et al., 2015; Hauer et al., 2017). However, the experimental quantification of the impact of hydropeaking on solute transport, mixing, and mixing enhancement in the underlying aquifer has received little attention.

This work provides experimental evidence of the effects of hydropeaking on solute transport and mixing enhancement in porous aquifers. We adopt an approach based on multidimensional flow-through experiments, which have been increasingly used to investigate solute transport and mixing in steady-state flow fields (e.g., Castro-Alcalá et al., 2012; Haberer et al., 2015; Muniruzzaman & Rolle, 2015, 2017; Simmons et al., 2002; Ye et al., 2015b). Conversely, fewer contributions have provided experimental evidence of the effect of transient boundary conditions on mixing (e.g., Boufadel et al., 2007; Cho et al., 2019; Zhang et al., 2009), particularly in the context of surface water-groundwater interaction (Santizo et al., 2020). We focus on groundwater plume spreading and mixing enhancement caused by fluctuating stages in two river transects in hydraulic contact with the aquifer. Such setup was inspired by the conditions typically encountered in the Alps, where multiple streams in the same plain are affected by the operation of different hydropower plants (Pérez Ciria et al., 2019) and it is also representative of a longitudinal cross section of a meandering or braided river affected by a hydropeaking wave. We perform the experiments in a quasi-two-dimensional flow-through chamber representing the vertical cross-section of an unconfined homogeneous aquifer. The homogeneous porous medium allowed us to study the impact of transient flows caused by hydropeaking on solute transport and mixing in isolation, avoiding mixing enhancement effects that occur in heterogenous porous materials (e.g., Rolle et al., 2009; Werth et al., 2006; Ye et al., 2015c). A dye tracer is injected into the setup in a series of five experiments considering both steady and transient flows. High-resolution monitoring of the spatio-temporal plume evolution is performed with a non-invasive imaging technique and by depth-resolved sampling and spectrophotometric measurements at the outlet of the setup. We quantify plume spreading and mixing, and their link with the highly fluctuating flow fields by analyzing breakthrough curves (BTCs), the second central spatial moments of the solute distribution, the dilution index, and the flux-related dilution index.

2. Experimental Setup

A quasi 2-D acrylic glass setup with inner dimensions of $77.9 \times 15 \times 1.1$ cm^3 (length × height × width) was used as a flow-through chamber (Figure 1). The experiments were performed in an unconfined homogenous porous medium made of glass beads with a diameter in the range 1.0–1.5 mm (Sartorius AG, Germany).

In the transient flow experiments, an additional layer of sand (d = 0.5–0.8 mm, Euroquartz, Germany) was positioned on top of the glass beads to recreate the riverbed and the riverbanks. The riverbed bottoms of the

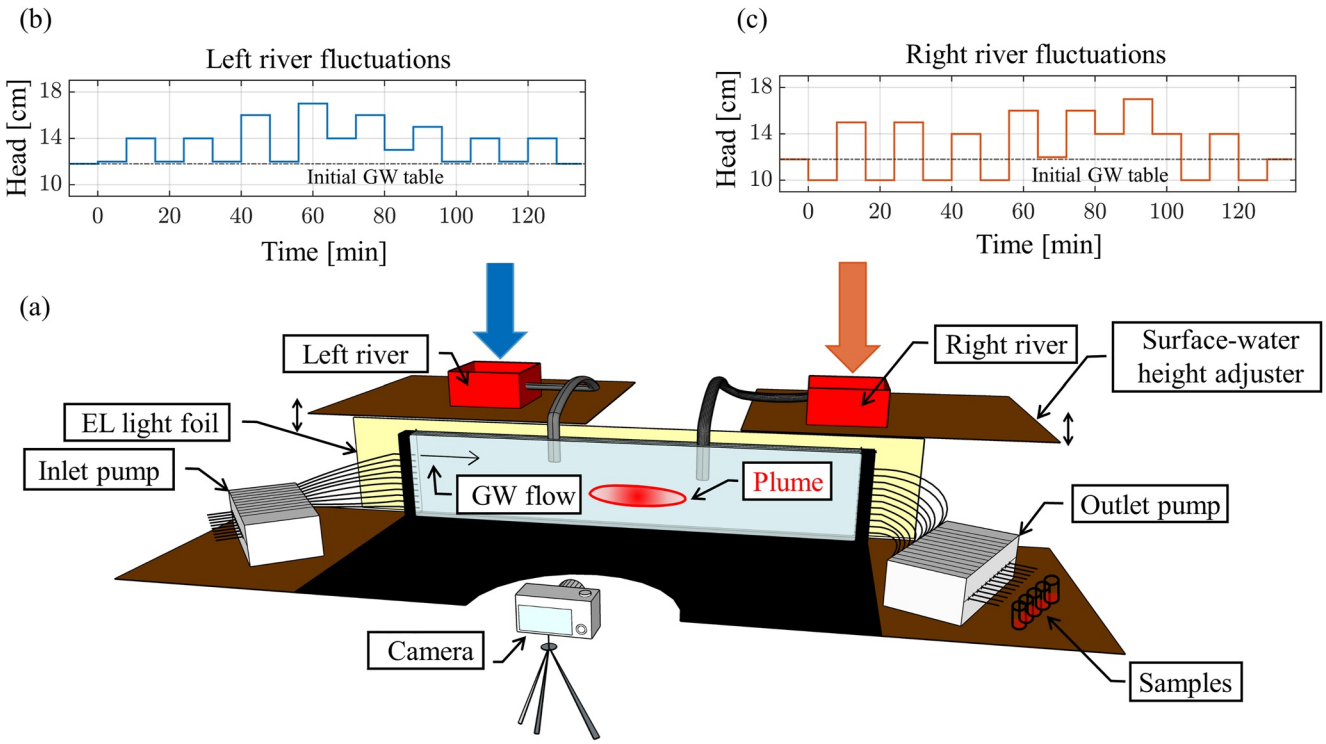

Figure 1. (a) Schematic illustration of the experimental setup, including the flow-through chamber, the inlet, and outlet pumps, and the reservoirs placed above two surface-water height adjusters mimicking hydropeaking. (b–c) Hydrographs showing the fluctuations of the two rivers used in one of the transient flow experiments (Transient 1).

two river transects were placed at different depths in the flow-through chamber to allow for both losing (left river) and variably losing/gaining conditions (right river), moreover, the rivers have different widths and riverbed thickness as indicated in Table S1. The flow-through the system is equipped with 13 ports, equally spaced by a constant distance of 1.1 cm. Two high-precision multi-channel peristaltic pumps (IPC-N24, ColeParmer, United States) were connected to the lowest 10 inlet and outlet ports to establish the flow in the aquifer. To generate transient flow conditions within the porous medium, two water reservoirs were connected to the top of the flow-through chamber with two semi-rigid tubes and placed on two surface-water height adjusters, which could be moved vertically to simulate an oscillating water head (Figure 1). An additional channel was considered at the outlet to avoid the overflow of the system due to the additional water from the losing conditions of the rivers in the transient experiments. The river stage fluctuations are shown in Figure 1.

In the experiments we consider river-aquifer interaction by changing the phase of the oscillations in the stage of the two rivers, the amplitude of the fluctuations, the river bottom location, the thickness of the sandy river bottom, and the width of the two rivers. The frequency of the oscillations is kept constant. In the transient experiments, the Townley number (i.e., ratio between the relative time scale of diffusion and the tidal forcing), and the tidal strength (i.e., ratio between the amplitude of the tidal forcing and the regional gradient) are typical for systems affected by hydropeaking (Francis et al., 2010; Sawyer et al., 2009; Pérez Ciria et al., 2019) and coastal aquifers (e.g.., Trefry et al., 2019) and are reported in the Text S1, Table S1 and Figure S1 in Supporting Information S1. The grain Péclet number of the experiment is 566 and indicates advection-dominated conditions. During each experiment, a constant concentration $C_0 = 300$ mg/L of the red azo dye new coccine (CAS 2611-82-7, Sigma-Aldrich, United States) solution was injected from the two central inlet ports (fourth and fifth) for 24 min. This tracer is chemically stable and photostable and displays low scattering and no fluorescence (Jaeger et al., 2009). The plume movement and concentration were captured with optical imaging, using a Nikon D5000 camera (12 Megapixel resolution, 18–55 mm Nikon lens). Details about the optical calibration are provided in Text S2 and Figures S2 and S3. We collected samples at the outlet ports every 4 min (~120 samples for each experiment) and measured the tracer concentration

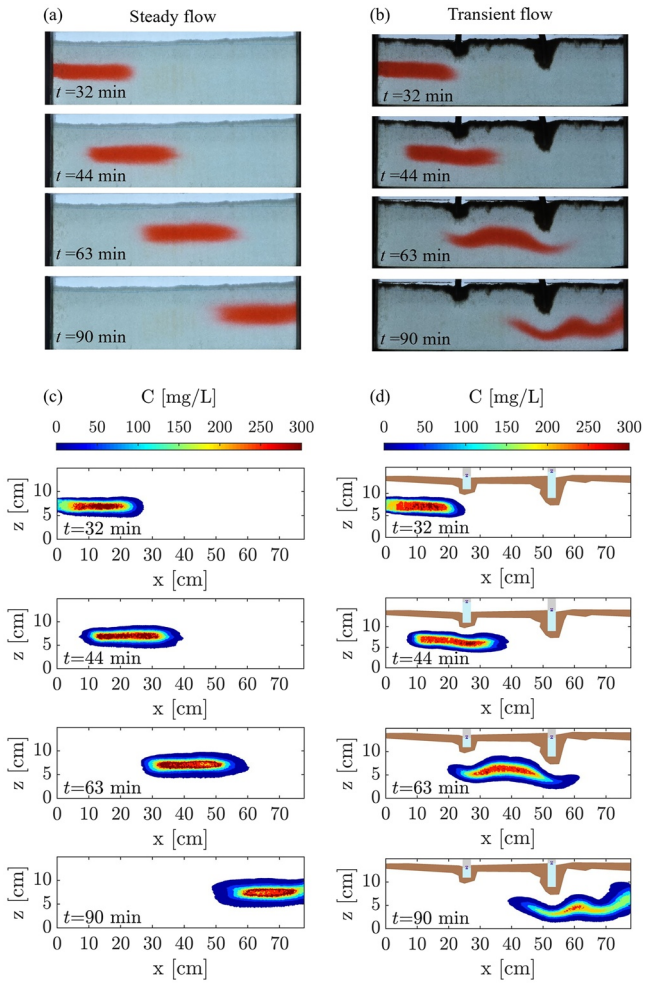

Figure 2. Photographs (a–b) and processed images (c–d) of the dye tracer plume at different time steps under steady and transient flow conditions.

using a DR 3900 Spectrophotometer (Hach Lange, Germany). The collected samples were also used to validate the results obtained from the optical analysis and to calculate the flux-related dilution index. The spectroscopy calibration curve is shown in Figure S4.

We processed the raw images taken with the camera to quantify the concentration of the tracer using an algorithm based on the one presented by Jaeger et al. (2009). A comparison between raw photographs and post-processed images is shown in Figure 2 for four plume pictures at different time steps (Figures 2a and 2b) and the mapped concentrations (Figures 2c and 2d) under steady and transient flow conditions.

The photographs in Figure 2 highlight the difference in the plume shape between the steady and transient setups while the tracer plume moves through the porous medium. A deformed plume in the transient experiment (Figure 2b) is observed as a consequence of the interaction with the rivers. Besides capturing the evolving shape of the plume, the post-processed images (Figures 2c and 2d) allowed us to quantify the temporal evolution of solute concentrations, which is necessary for the analysis of spreading and mixing in each experiment.

A total of five flow-through experiments was performed. The first one was run under steady-state flow conditions without the river system. In the second experiment, the rivers were added to the previous setup, keeping the head of both rivers equal to the groundwater table to avoid any surface water - groundwater exchange. Finally, three transient flow experiments were performed considering two time series of fluctuating river heads (Figure 1). In the first transient experiment, the head fluctuations in the left and right rivers were in-phase, while in the second one they were in counter-phase. In the third transient flow experiment, the river fluctuations in counter-phase were repeated by filling with sand the whole part of the flow-through chamber above the glass beads, to reduce the possible occurrence of water levels higher than the porous matrix and in this way lowering the centroid of the plume in the vertical direction after injection of the tracer solution (Figure S8). Details of the experimental settings, river fluctuations, and hydraulic and transport parameters are reported in Table S1 while the dataset is available in Ziliotto et al. (2021).

3. Evaluation of Plume Spreading and Mixing

We computed the spatial moments to analyze the distribution of the solute concentration in the porous medium and to quantify the spreading of the plume and its temporal evolution. The first spatial moment in the i- direction, $\boldsymbol{\alpha_i}$ [L], is used to describe the location of the centroid of the plume and it is calculated as:

$$\boldsymbol{\alpha_i}(t) = \int_V p(\boldsymbol{x},t)\, x_i\, dV \tag{1}$$

where x_i is the i^{th} component of the spatial coordinates, t is a dimensionless time expressed in pore volumes ($PV = (v\,t)/L$, where v is the seepage velocity and L is the length of the flow-through chamber), and $p\,(x,t)$ [L^{-3}] is the probability distribution of the location of the tracer at time t in the domain V:

$$p(\boldsymbol{x},t) = \frac{c(\boldsymbol{x},t)}{\int_V c(\boldsymbol{x},t)\, dV} \tag{2}$$

The second spatial moment $\boldsymbol{\Delta_{ij}}$ [L^2] is a second-order tensor and represents the mean square distance from the centroid of the plume. It gives information about the spreading of the plume and it is computed as:

$$\boldsymbol{\Delta_{ij}}(t) = \int_V p(\boldsymbol{x},t)(x_i - \alpha_i)(x_j - \alpha_j)dV \tag{3}$$

A dimensionless second spatial moment is obtained by dividing the value of $\boldsymbol{\Delta_{ij}}(t)$ by $\boldsymbol{\Delta_{ij}}(t_p)$, where t_p is the time at which the tracer solution is completely injected in the flow-through setup. To evaluate mixing in porous media, we computed the dilution index (Kitanidis, 1994) and the flux-related dilution index (Chiogna et al., 2011; Rolle & Kitanidis, 2014). The dilution index $E(t)$ [L^3] is related to the Shannon entropy of the concentration of a plume and is a true measure of mixing that is expressed by the following equation:

$$E(t) = exp\left(-\int_V p(\boldsymbol{x},t)\ln\left(p(\boldsymbol{x},t)\right)dV\right) \tag{4}$$

The dimensionless representation of the dilution index is called volumetric reactor ratio M and it is obtained by dividing the dilution index by the volume of the flow-through system. The flux-related formulation of the dilution index, $E_Q(x,t)$, can also be used to characterize mixing in flow-through porous media. This metric quantifies how the mass flux of a solute is distributed over a given flow rate (Chiogna et al., 2011; Rolle et al., 2009) and it is calculated as (Rolle & Kitanidis, 2014):

$$E_Q(\boldsymbol{x},t) = exp\left(-\int_A p_Q(\boldsymbol{x},t)\ln\left(p_Q(\boldsymbol{x},t)q_x(\boldsymbol{x},t)\right)dA\right) \tag{5}$$

where $q_x(x,t)$ [L/T] is the component of the specific discharge in the main flow direction, A [L^2] is the cross-sectional area normal to the main flow direction and $p_Q(x,t)$ is the flux-related probability density function of the concentration:

$$p_Q(\boldsymbol{x},t) = \frac{c(\boldsymbol{x},t)}{\int_A c(\boldsymbol{x},t)q_x(\boldsymbol{x},t)dA} \tag{6}$$

The dimensionless representation of the flux-related dilution index is obtained by dividing $\boldsymbol{E_Q}(\boldsymbol{x},\boldsymbol{t})$ by the water flux through the system.

4. Results and Discussion

The experiments performed in this study allowed investigating the dynamics of spreading and mixing of a plume affected by the transient fluctuations occurring in the river stage due to hydropeaking. Such fluctuations have an important impact both on the solute breakthrough at the outlet of the setup and on the concentration distribution within the porous medium.

4.1. Breakthrough Curves

The quantification of solute concentration at the outlet of the flow-through chamber allowed obtaining port-resolved (Figure 3) and integrated BTCs (Figure S6). The BTCs of new coccine at several outlet ports reported in Figure 3 show the results of transport under steady flow conditions and under the fluctuating conditions of the transient flow 1 experiment. Similar results for the other transient experiments are reported in Figures S5 and S6, showing that considering both in-phase or counter-phase oscillations leads to multi-peaked BTCs.

In the steady flow field, the solute plume displays the typical bell-shaped concentration distribution at all ports, and the highest peak concentrations occur at ports 4 and 5, which are in line with the injection of the plume at the inlet. The breakthrough curves of the transient flow 1 experiment display more complex patterns. As observed in Figure 2, the transient flow, induced by the fluctuations in the river stage, leads to stretching and folding, enhanced spreading in the longitudinal and transverse directions, and also depth-dependent variations of the advective velocity. The part of the plume closer to the river is more affected by the change in the hydraulic head gradients and shows more pronounced deformation in the concentration distribution within the porous medium. The breakthrough curves measured in the transient experiments become multi-modal, especially in the core of the plume (ports 4, 5, 6, and 7); normalized concentrations higher than 0.5 occur now at three ports (ports 5, 6, and 7) at three distinct times (1.12 PV, 1.32 PV, and 1.28 PV, respectively) and we can observe strong fluctuations in the concentration values measured at the same port at different times. Besides the concentration values of the measured breakthrough curves, the river stage fluctuations also impact the time at which peak concentrations are reached. The first peak concentration occurs earlier in the transient experiment than the single peak displayed in the steady flow experiment. In

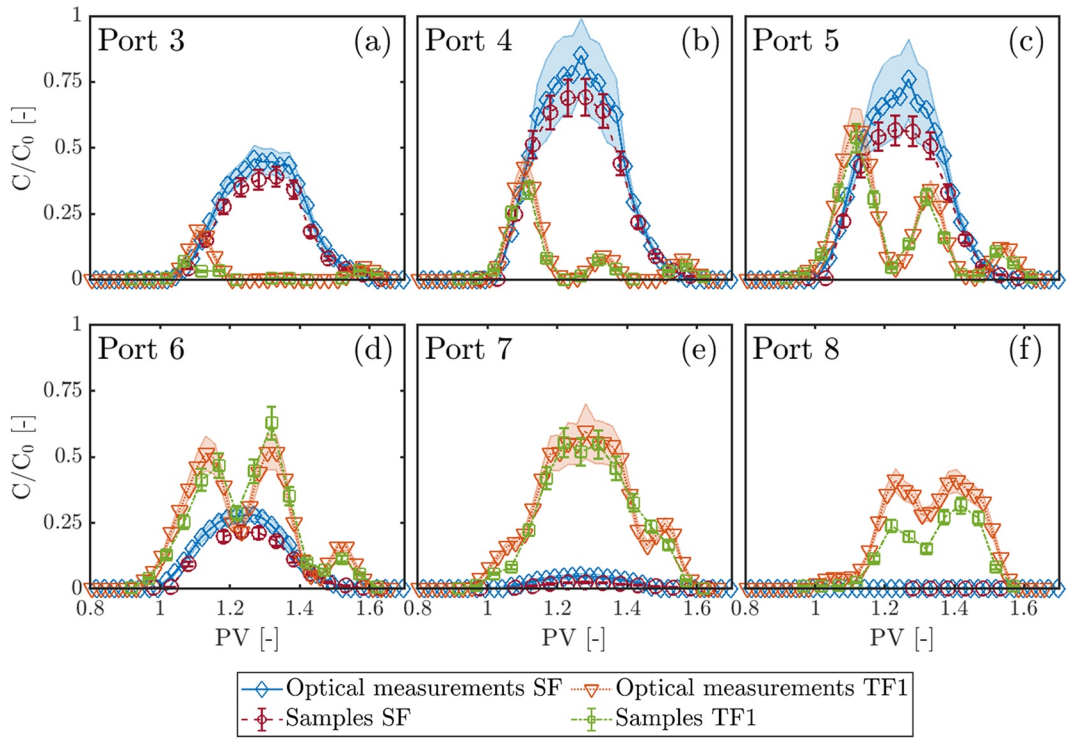

Figure 3. Breakthrough curves obtained from the results of the optical analysis and spectrophotometric measurements of the samples collected at different outlet ports in a steady flow and transient flow Experiment 1 (TF1). The shaded areas represent the experimental uncertainty of the concentration estimated by image analysis.

fact, the mean velocity increases due to the local reduction of the thickness of the saturated porous medium induced by the presence of the rivers (this effect is clearly visible in the breakthrough curves measured for the steady flow experiment with rivers in Figure S5). Moreover, positive and negative fluctuations around the mean flow velocity caused by changes in the river stage can both accelerate and decelerate the plume movement (depending on its location in the system), increase spreading in the longitudinal direction, and influence local dispersion by sharpening concentration gradients and by affecting the magnitude of the hydrodynamic dispersion coefficients. We provide further details and data about a solute breakthrough in the Supporting Information S1, including the port-resolved breakthrough curves for all experiments (Figure S5), the depth-integrated breakthrough curves (Figure S6), and the evolution of the vertical spatial profiles at the outlet for the steady flow and the transient flow Experiment 1 (Figure S7). Considering the location of the first central moment on the vertical direction through the comparison between Transient 2 and Transient 3 experiments, we can observe that the multi-modal shape of the BTCs is more pronounced in plumes that flow closer to the river boundary (Figures S5 and S8).

4.2. Plume Spreading, Mixing, and Mixing Enhancement

The normalized second moments in the longitudinal and transverse directions, $\Delta_{xx}(t)/\Delta_{xx}(t_p)$ and $\Delta_{zz}(t)/\Delta_{zz}(t_p)$, respectively, and the volumetric reactor ratio M for all flow-through experiments were computed based on the results of the image analysis (Figures 4a–4c). The flux-related reactor ratio, M_Q (Figure 4d), was calculated from the collected samples at the outlet using the flow rate measured at each port and the samples' solute concentrations determined by spectrophotometric analysis. These quantities were calculated to analyze and quantify the impact of the rivers' fluctuations on plume spreading, mixing, and mixing enhancement. In addition to the experimental results of the steady flow experiment, we computed the analytical solution of the 2-D advection-dispersion equation considering a pulse input of a tracer from a line source (Text S3). Even if the analytical solution requires some simplifications in comparison to the

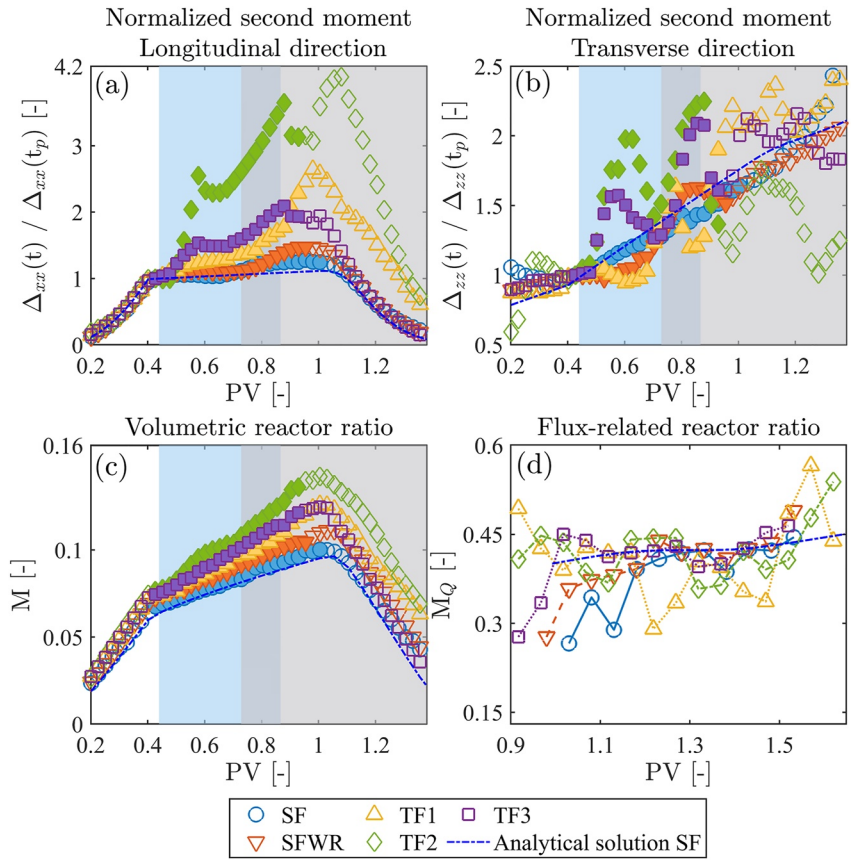

Figure 4. Second spatial moments normalized by $\mathbf{\Delta}_{ij}(t_p)$, where t_p is the time at which the tracer solution is completely injected in the flow-through setup, obtained from the optical analysis for all the experiments (a–b). Volumetric reactor ratio M obtained from the optical analysis for all the experiments (c). The filled markers indicate the time during which the tracer solution is completely injected in the flow-through setup. The light blue area (fx5) indicates the time spent by the plume under the left river, while the gray area (fx6) indicates the time spent under the right river. Panel (d) shows the flux-related reactor ratio obtained from the spectrophotometric analysis of the samples collected at the outlet of the setup.

experimental setup, it describes very well the steady flow experiment without rivers, validating the evidence collected in the steady flow experiments and allowing the quantification of local longitudinal and transverse dispersion coefficients ($D_{l,sf} = 1.02 \times 10^{-7}$ m^2/s and $D_{t,sf} = 8.0 \times 10^{-9}$ m^2/s).

Figures 4a and 4b show that the spreading in the longitudinal and transverse directions is more pronounced in the transient flow experiments than in the steady flow ones. The spreading in the longitudinal direction increases following almost a monotonic trend for all the experiments. However, we can observe the different effect of a loosing river (left river) in comparison to a loosing/gaining river (right river). The increase in longitudinal spreading is reduced under loosing conditions since the longitudinal flow velocity of the plume decreases. If loosing/gaining conditions are variably present, longitudinal spreading decreases/increases due to the river acting as a source/sink term for the flow. On the contrary, the spreading in the transverse direction fluctuates strongly in accordance with the squeezing and the stretching of the plume caused by the oscillations in the rivers' water table. The highest and fastest increase in spreading occurs below the river on the right, where the shape of the plume significantly changes. The downstream river is located deeper than the one upstream and is characterized by stage fluctuations with a larger amplitude. Therefore, the closer the plume is to the surface water-groundwater interface and the larger the fluctuations, the larger is the expected effect of hydropeaking on spreading. For instance, the comparison between transient 2 and transient 3 experiments close to the left river shows that the amplitude in the fluctuations of Δ_{zz} is related to the distance of the centroid of the plume to the river (Figure S8). Comparing the differences in the timing of the peaks in Δ_{zz}, we can appreciate the effect of the phase shift between the oscillations in transient 1

(in-phase), and transient 2 and transient 3 (counter-phase) experiments. Moreover, during transient flow conditions, local transverse dispersion, which is nonlinearly dependent on the groundwater flow velocity (Chiogna et al., 2010), may have an additional effect on enhancing spreading in the vertical direction (Figure 4b). Even if mixing cannot be described by the second moments only, a correlation between spreading in the vertical direction and mixing can be observed. In fact, the dilution index increases faster under transient flow than in steady flow conditions (Figure 4c). As observed, the spatial variability of the flow velocity leads to changes of plume shape, enhances solute spreading, affects local dispersion coefficients, and all these processes result in enhancement of plume dilution. Finally, we observe that the hydropeaking-induced fluctuations impact the distribution of the solute mass flux over the water flux (Figure 4d). The flux-related reactor ratio integrates both the impact on solute distribution by diffusive-dispersive processes at the plume fringe as well as the changing water flux due to the hydraulic connection of the rivers with the underlying aquifer. Overall, the fluctuations cause a distribution of the solute over a larger flow rate in particular at early and late times (i.e., 0.92 PV $< t <$ 1.12 PV and 1.47 PV $< t <$ 1.62 PV, respectively) when higher values of flux-related reactor ratio are reached. This behavior is explained by the fact that plumes in the transient experiments are more elongated than in the steady flow experiments and the forward and backward fringes of the plume are more diluted. Spreading and mixing enhancement show very dynamic patterns, which are illustrated in Figures S9–S11. The sole presence of the rivers leads to some increase of Δ_{xx} and Δ_{zz} (i.e., 20.4% and 49.8%, respectively) as shown in Figures S9 and S10, and only to a slight mixing enhancement of 4.8% at the outlet of the system (Figure S11). All transient flow experiments show significant spreading enhancement (Δ_{xx} from 63% to 105.6% and Δ_{zz} from 81.9% to 249.5%) and mixing enhancement ranging from 23.7% to 41.8% at the end of the system, with respect to the steady flow experiment. More specifically, the spreading enhancement only due to hydropeaking (i.e., compared with the steady flow with rivers experiment) ranges from Δ_{xx} 44.7% to 78.8% and from Δ_{zz} 38.7% to 209.6%, and the mixing enhancement ranges from 13.2% to 29.7% at the outlet of the flow-through chamber. In the transient flow Experiment 1, we observe the smallest maximum enhancement in lateral spreading (i.e., 81.9%) and consequently the smallest mixing enhancement (23.7%). Conversely, when Δ_{zz} reaches its maximum value in the transient flow Experiment 2 (249.5% at 0.43 PV), we observe a variation in the slope of the volumetric reactor ratio (Figures 4b and 4c), and the highest increment (+41.8%) is reached at the outlet of the system (Figures S10 and S11). These results show a positive correlation between plume deformation quantified through lateral spreading and mixing enhancement. In particular, from the analyzed setups we can observe that the distance of the plume to the riverbed and the amplitude of the fluctuations are key factors controlling mixing and spreading, whereas the phase shift between the fluctuations of the two rivers and the thickness of the sand layer plays a minor role. Finally, Figure S12 shows that our system does not reach an asymptotic value in the effective dispersion coefficient as, for example, in Bolster et al. (2009), Dentz and Carrera (2005), and de Dreuzy et al. (2012) due to the local impact of the river fluctuations and their high frequency. In our experiment, the system remains in non-equilibrium conditions, and the mean values of both longitudinal and transverse effective dispersion coefficients, normalized by $D_{\mathrm{l,sf}}$ and $D_{\mathrm{t,sf}}$, vary with the river fluctuations.

5. Conclusions

The laboratory investigation performed in this study provides the first experimental evidence of the effects of dynamic river fluctuations, mimicking hydropeaking conditions, on solute transport and concentration distribution in the subsurface. The experimental outcomes, obtained by combining high-resolution imagining techniques and conventional depth-resolved sampling and spectrophotometric analysis, show that hydropeaking generates multi-modal, fluctuating breakthrough curves. Our results also show a significant spreading and mixing enhancement when comparing the transient flow with the steady flow experiments. Moreover, the unique dataset collected in this experimental investigation can be used in future studies to test theoretical works on plume dispersion in porous media, as well as the capabilities of numerical models to accurately describe flow and transport under transient conditions. The rivers' fluctuations enhance spreading in the longitudinal direction and cause the spreading in the vertical direction to strongly fluctuate because of the squeezing and the stretching of the plume. Even if spreading cannot univocally describe mixing, the link between the spreading in the vertical direction and mixing enhancement is evident. In fact, when the plume is more deformed and consequently diffusive/dispersive fluxes occur over a larger area, mixing is also enhanced. These findings are opposite to the observations in heterogeneous media, where

mixing enhancement is mainly caused by flow focusing: in regions of high hydraulic conductivity contrast, streamlines are squeezed and the area available for diffusive/dispersive fluxes decreases (i.e., a reduction in transverse spreading), however, the solute distributes effectively over a larger water flux. Indeed, the main mixing enhancement in the setup considered in this study is due to an increase in plume spreading and to changes in the local dispersion coefficient caused by the highly transient boundary conditions. Our outcomes show the importance of considering hydropeaking, and more generally transient conditions at the surface water-groundwater interface, as an important factor for subsurface solute transport.

Data Availability Statement

Datasets for this research are available in this in-text data citation reference: Ziliotto et al. (2021). "Mixing enhancement mechanisms in aquifers affected by hydropeaking: Insights from flow-through laboratory experiments. Mendeley Data, V2, https://doi.org/10.17632/sx9gj2mhhm.2, www.doi.org/10.17632/sx9gj2mhhm.2.

Acknowledgments
This collaborative research is a result of the UNMIX project (UNcertainties due to boundary conditions in predicting MIXing in groundwater), which is supported by the Deutsche Forschungsgemeinschaft (DFG) through the TUM International Graduate School for Science and Engineering (IGSSE), GSC 81. Financial support for initiating the collaboration was provided by the Bayerische Forschungsallianz (BayFOR) GmbH, through the Bayerischen Hochschulförderprogramms zur Anbahnung internationaler Forschungskooperationen (BayIntAn_TUM_2019_65). MBH also acknowledges the support of the Mexican National Council for Science and Technology (CONACYT) and the Consejo Veracruzano de Investigación Científica y Desarrollo Tecnológico (COVEICYDET). Additional financial support for GC was provided by DFG in the Project Hydromix (CH 981/4-1). Open access funding enabled and organized by Projekt DEAL.

References

Aref, H., Blake, J. R., Budišić, M., Cardoso, S. S. S., Cartwright, J. H. E., Clercx, H. J. H., et al. (2017). Frontiers of chaotic advection. *Reviews of Modern Physics*, *89*(2), 025007. https://doi.org/10.1103/RevModPhys.89.025007

Bagtzoglou, A. C., & Oates, P. M. (2007). Chaotic advection and enhanced groundwater remediation. *Journal of Materials in Civil Engineering*, *19*, 75–83. https://doi.org/10.1061/(ASCE)0899-1561(2007)19:1(75)

Bandopadhyay, A., Davy, P., & Le Borgne, T. (2018). Shear flows accelerate mixing dynamics in hyporheic zones and hillslopes. *Geophysical Research Letters*, *45*(21), 11,659–11,668, 11. https://doi.org/10.1029/2018GL079914

Bauer, R. D., Rolle, M., Bauer, S., Eberhardt, C., Grathwohl, P., Kolditz, O., et al. (2009). Enhanced biodegradation by hydraulic heterogeneities in petroleum hydrocarbon plumes. *Journal of Contaminant Hydrology*, *105*(1–2), 56–68. https://doi.org/10.1016/j.jconhyd.2008.11.004

Béjar, M., Vericat, D., Batalla, R. J., & Gibbins, C. N. (2018). Variation in flow and suspended sediment transport in a montane river affected by hydropeaking and instream mining. *Geomorphology*, *310*, 69–83. https://doi.org/10.1016/j.geomorph.2018.03.001

Bolster, D., Dentz, M., & Carrera, J. (2009). Effective two-phase flow in heterogeneous media under temporal pressure fluctuations. *Water Resources Research*, *45*(5). https://doi.org/10.1029/2008WR007460

Boufadel, M., Li, H., Suidan, M., & Venosa, A. (2007). Tracer studies in a laboratory beach subjected to waves. *Journal of Environmental Engineering*, *133*(7), 722–732. https://doi.org/10.1061/(ASCE)0733-9372(2007)133:7(722)

Cardenas, M. B., Wilson, J. L., & Zlotnik, V. A. (2004). Impact of heterogeneity, bed forms, and stream curvature on subchannel hyporheic exchange. *Water Resources Research*, *40*(8), W08307. https://doi.org/10.1029/2004WR003008

Castro-Alcalá, E., Fernàndez-Garcia, D., Carrera, J., & Bolster, D. (2012). Visualization of mixing processes in a heterogeneous sand box aquifer. *Environmental Science & Technology*, *46*(6), 3228–3235. https://doi.org/10.1021/es201779p

Chiogna, G., Cirpka, O. A., Grathwohl, P., & Rolle, M. (2011). Transverse mixing of conservative and reactive tracers in porous media: Quantification through the concepts of flux-related and critical dilution indices. *Water Resources Research*, *47*(2), W02505. https://doi.org/10.1029/2010WR009608

Chiogna, G., Cirpka, O. A., Rolle, M., & Bellin, A. (2015). Helical flow in three-dimensional nonstationary anisotropic heterogeneous porous media. *Water Resources Research*, *51*, 261–280. https://doi.org/10.1002/2014WR015330

Chiogna, G., Eberhardt, C., Grathwohl, P., Cirpka, O. A., & Rolle, M. (2010). Evidence of compound-dependent hydrodynamic and mechanical transverse dispersion by multitracer laboratory experiments. *Environmental Science & Technology*, *44*(2), 688–693. https://doi.org/10.1021/es9023964

Chiogna, G., Hochstetler, D. L., Bellin, A., Kitanidis, P. K., & Rolle, M. (2012). Mixing, entropy and reactive solute transport. *Geophysical Research Letters*, *39*, L20405. https://doi.org/10.1029/2012gl053295

Cho, M. S., Solano, F., Thomson, N. R., Trefry, M. G., Lester, D. R., & Metcalfe, G. (2019). Field trials of chaotic advection to enhance reagent delivery. *Groundwater Monitoring & Remediation*, *39*(3), 23–39. https://doi.org/10.1111/gwmr.12339

Cil, M. B., Xie, M., Packman, A. I., & Buscarnera, G. (2017). Solute mixing regulates heterogeneity of mineral precipitation in porous media. *Geophysical Research Letters*, *44*, 6658–6666. https://doi.org/10.1002/2017GL073999

de Anna, P., Dentz, M., Tartakovsky, A., & LeBorgne, T. (2014). The filamentary structure of mixing fronts and its control on reaction kinetics in porous media flows. *Geophysical Research Letters*, *41*, 4586–4593. https://doi.org/10.1002/2014GL060068

de Barros, F. P. J., Dentz, M., Koch, J., & Nowak, W. (2012). Flow topology and scalar mixing in spatially heterogeneous flow fields. *Geophysical Research Letters*, *39*, L08404. https://doi.org/10.1029/2012GL051302

de Dreuzy, J.-R., Carrera, J., Dentz, M., & Le Borgne, T. (2012). Asymptotic dispersion for two-dimensional highly heterogeneous permeability fields under temporally fluctuating flow. *Water Resources Research*, *48*, W01532. https://doi.org/10.1029/2011wr011129

Dentz, M., & Carrera, J. (2003). Effective dispersion in temporally fluctuating flow through a heterogeneous medium. *Physical Review. E, Statistical, nonlinear, and soft matter physics*, *68*(3 Pt 2), 036310. https://doi.org/10.1103/PhysRevE.68.036310

Dentz, M., & Carrera, J. (2005). Effective solute transport in temporally fluctuating flow through heterogeneous media. *Water Resources Research*, *41*, W08414. https://doi.org/10.1029/2004WR003571

Dentz, M., Lester, D. R., Le Borgne, T., & de Barros, F. P. J. (2016). Coupled continuous-time random walks for fluid stretching in two-dimensional heterogeneous media. *Physical Review E*, *94*(6). https://doi.org/10.1103/PhysRevE.94.061102

Ferencz, S. B., Cardenas, M. B., & Neilson, B. T. (2019). Analysis of the effects of dam release properties and ambient groundwater flow on surface water-groundwater exchange over a 100-km-long reach. *Water Resources Research*, *55*, 8526–8546. https://doi.org/10.1029/2019WR025210

Francis, B. A., Francis, L. K., & Cardenas, M. B. (2010). Water table dynamics and groundwater–surface water interaction during filling and draining of a large fluvial island due to dam-induced river stage fluctuations. *Water Resources Research*, *46*, W07513. https://doi.org/10.1029/2009WR008694

Geng, X., Michael, H. A., Boufadel, M. C., Molz, F. J., Gerges, F., & Lee, K. (2020). Heterogeneity affects intertidal flow topology in coastal beach aquifers. *Geophysical Research Letters*, *47*, e2020GL089612. https://doi.org/10.1029/2020GL089612

Gillespie, B. R., Desmet, S., Kay, P., Tillotson, M. R., & Brown, L. E. (2015). A critical analysis of regulated river ecosystem responses to managed environmental flows from reservoirs. *Freshwater Biology*, *60*, 410–425. https://doi.org/10.1111/fwb.12506

Haberer, C. M., Muniruzzaman, M., Grathwohl, P., & Rolle, M. (2015). Diffusive–dispersive and reactive fronts in porous media: Iron(II) oxidation at the unsaturated–saturated interface. *Vadose Zone Journal*, *14*, 1–14. https://doi.org/10.2136/vzj2014.07.0091

Hauer, C., Holzapfel, P., Leitner, P., & Graf, W. (2017). Longitudinal assessment of hydropeaking impacts on various scales for an improved process understanding and the design of mitigation measures. *The Science of the Total Environment*, *575*, 1503–1514. https://doi.org/10.1016/j.scitotenv.2016.10.031

Hester, E. T., Cardenas, M. B., Haggerty, R., & Apte, S. V. (2017). The importance and challenge of hyporheic mixing. *Water Resources Research*, *53*, 3565–3575. https://doi.org/10.1002/2016wr020005

Hester, E. T., Young, K. I., & Widdowson, M. A. (2013). Mixing of surface and groundwater induced by riverbed dunes: Implications for hyporheic zone definitions and pollutant reactions. *Water Resources Research*, *49*, 5221–5237. https://doi.org/10.1002/wrcr.20399

Heyman, J., Lester, D. R., Turuban, R., Méheust, Y., & Le Borgne, T. (2020). Stretching and folding sustain microscale chemical gradients in porous media. *Proceedings of the National Academy of Sciences*, *117*(24), 13359–13365. https://doi.org/10.1073/pnas.2002858117

Jaeger, S., Ehni, M., Eberhardt, C., Rolle, M., Grathwohl, P., & Gauglitz, G. (2009). CCD camera image analysis for mapping solute concentrations in saturated porous media. *Analytical and Bioanalytical Chemistry*, *395*(6), 1867–1876. https://doi.org/10.1007/s00216-009-2978-3

Jiménez-Martínez, J., Porter, M. L., Hyman, J. D., Carey, J. W., & Viswanathan, H. S. (2016). Mixing in a three-phase system: Enhanced production of oil-wet reservoirs by CO_2 injection. *Geophysical Research Letters*, *43*, 196–205. https://doi.org/10.1002/2015GL066787

Kahler, D. M., & Kabala, Z. J. (2016). Acceleration of groundwater remediation by deep sweeps and vortex ejections induced by rapidly pulsed pumping. *Water Resources Research*, *52*, 3930–3940. https://doi.org/10.1002/2015WR017157

Kitanidis, P. K. (1994). The concept of the Dilution Index. *Water Resources Research*, *30*(7), 2011–2026. https://doi.org/10.1029/94WR00762

Lester, D., Dentz, M., & Le Borgne, T. (2016). Chaotic mixing in three-dimensional porous media. *Journal of Fluid Mechanics*, *803*, 144–174. https://doi.org/10.1017/jfm.2016.486

Lester, D. R., Metcalfe, G., & Trefry, M. G. (2013). Is chaotic advection inherent to porous media flow? *Physical Review Letters*, *111*(17), 174101. https://doi.org/10.1103/PhysRevLett.111.174101

Maavara, T., Chen, Q., Van Meter, K., Brown, L. E., Zhang, J., Ni, J., & Zarfl, C. (2020). River dam impacts on biogeochemical cycling. *Nature Reviews Earth & Environment*, *1*, 103–116. https://doi.org/10.1038/s43017-019-0019-0

Muniruzzaman, M., & Rolle, M. (2015). Impact of multicomponent ionic transport on pH fronts propagation in saturated porous media. *Water Resources Research*, *51*, 6739–6755. https://doi.org/10.1002/2015WR017134

Muniruzzaman, M., & Rolle, M. (2017). Experimental investigation of the impact of compound-specific dispersion and electrostatic interactions on transient transport and solute breakthrough. *Water Resources Research*, *53*, 1189–1209. https://doi.org/10.1002/2016WR019727

Neupauer, R. M., Meiss, J. D., & Mays, D. C. (2014). Chaotic advection and reaction during engineered injection and extraction in heterogeneous porous media. *Water Resources Research*, *50*, 1433–1447. https://doi.org/10.1002/2013WR014057

Ottino, J. M. (1990). Mixing, chaotic advection, and turbulence. *Annual Review of Fluid Mechanics*, *22*(1), 207–254. https://doi.org/10.1146/annurev.fl.22.010190.001231

Pérez Ciria, T., Labat, D., & Chiogna, G. (2019). Detection and interpretation of recent and historical streamflow alterations caused by river damming and hydropower production in the Adige and Inn River basins using continuous, discrete and multiresolution wavelet analysis. *Journal of Hydrology*, *578*, 124021. https://doi.org/10.1016/j.jhydrol.2019.124021

Piscopo, A. N., Neupauer, R. M., & Mays, D. C. (2013). Engineered injection and extraction to enhance reaction for improved in situ remediation. *Water Resources Research*, *49*, 3618–3625. https://doi.org/10.1002/wrcr.20209

Pulg, U., Vollset, K. W., Velle, G., & Stranzl, S. (2016). First observations of saturopeaking: Characteristics and implications. *The Science of the Total Environment*, *573*, 1615–1621. https://doi.org/10.1016/j.scitotenv.2016.09.143

Reising, L., Neupauer, R., Mays, D. C., Crimaldi, J. P., & Roth, E. J. (2018). *Effects of active and Ppassive spreading on mixing and reaction during groundwater remediation by engineered injection and extraction. Civil engineering Graduate theses & Dissertations* (Vol. 414). University of Colorado Boulder.

Rodríguez-Escales, P., Fernàndez-Garcia, D., Drechsel, J., Folch, A., & Sanchez-Vila, X. (2017). Improving degradation of emerging organic compounds by applying chaotic advection in managed aquifer recharge in randomly heterogeneous porous media. *Water Resources Research*, *53*, 4376–4392. https://doi.org/10.1002/2016WR020333

Rolle, M., Chiogna, G., Hochstetler, D., & Kitanidis, P. (2013). On the importance of diffusion and compound-specific mixing for groundwater transport: An investigation from pore to field scale. *Journal of Contaminant Hydrology*, *153C*, 51–68. https://doi.org/10.1016/j.jconhyd.2013.07.006

Rolle, M., Eberhardt, C., Chiogna, G., Cirpka, O. A., & Grathwohl, P. (2009). Enhancement of dilution and transverse reactive mixing in porous media: Experiments and model-based interpretation. *Journal of Contaminant Hydrology*, *110*(3–4), 130–142. https://doi.org/10.1016/j.jconhyd.2009.10.003

Rolle, M., & Kitanidis, P. K. (2014). Effects of compound-specific dilution on transient transport and solute breakthrough: A pore-scale analysis. *Advances in Water Resources*, *71*, 186–199. https://doi.org/10.1016/j.advwatres.2014.06.012

Rolle, M., & Le Borgne, T. (2019). Mixing and reactive fronts in the subsurface. *Reviews in Mineralogy and Geochemistry*, *85*(1), 111–142. https://doi.org/10.2138/rmg.2018.85.5

Santizo, K. Y., Widdowson, M. A., & Hester, E. T. (2020). Abiotic mixing-dependent reaction in a laboratory simulated hyporheic zone. *Water Resources Research*, *56*(9), e2020WR027090. https://doi.org/10.1029/2020WR027090

Sawyer, A., Bayani Cardenas, M., Bomar, A., & Mackey, M. (2009). Impact of dam operations on hyporheic exchange in the riparian zone of a regulated river. *Hydrological Processes*, *23*(15), 2129–2137. https://doi.org/10.1002/hyp.7324

Schmadel, N. M., Ward, A. S., Lowry, C. S., & Malzone, J. M. (2016). Hyporheic exchange controlled by dynamic hydrologic boundary conditions. *Geophysical Research Letter*, *43*, 4408–4417. https://doi.org/10.1002/2016GL068286

Shuai, P., Chen, X., Song, X., Hammond, G. E., Zachara, J., Royer, P., et al. (2019). Dam operations and subsurface hydrogeology control dynamics of hydrologic exchange flows in a regulated river reach. *Water Resources Research*, *55*, 2593–2612. https://doi.org/10.1029/2018WR024193

Simmons, C., Pierini, M., & Hutson, J. (2002). Laboratory investigation of variable-density flow and solute transport in unsaturated–saturated porous media. *Transport in Porous Media*, *47*, 215–244. https://doi.org/10.1023/A:1015568724369

Singh, T., Gomez-Velez, J. D., Wu, L., Wörman, A., Hannah, D. M., & Krause, S. (2020). Effects of successive peak flow events on hyporheic exchange and residence times. *Water Resources Research*, *56*, e2020WR027113. https://doi.org/10.1029/2020WR027113

Sole-Mari, G., Fernàndez-Garcia, D., Sanchez-Vila, X., & Bolster, D. (2020). Lagrangian modeling of mixing-limited reactive transport in porous media: Multirate interaction by exchange with the mean. *Water Resources Research*, *56*, e2019WR026993. https://doi.org/10.1029/2019WR026993

Song, X., Chen, X., Stegen, J., Hammond, G., Song, H. S., Dai, H., et al. (2018). Drought conditions maximize the impact of high-frequency flow variations on thermal regimes and biogeochemical function in the hyporheic zone. *Water Resources Research*, *54*, 7361–7382. https://doi.org/10.1029/2018WR022586

Souzy, M., Lhuissier, H., Méheust, Y., Le Borgne, T., & Metzger, B. (2020). Velocity distributions, dispersion and stretching in three-dimensional porous media. *Journal of Fluid Mechanics*, *891*, A16. https://doi.org/10.1017/jfm.2020.113

Sposito, G. (2006). Chaotic solute advection by unsteady groundwater flow. *Water Resources Research*, *42*(6), W06D03. https://doi.org/10.1029/2005WR004518

Trefry, M. G., Lester, D. R., Metcalfe, G., & Wu, J. (2019). Temporal fluctuations and poroelasticity can generate chaotic advection in natural groundwater systems. *Water Resources Research*, *55*, 3347–3374. https://doi.org/10.1029/2018WR023864

Turuban, R., Lester, D. R., Heyman, J., Borgne, T. L., & Méheust, Y. (2019). Chaotic mixing in crystalline granular media. *Journal of Fluid Mechanics*, *871*, 562–594. https://doi.org/10.1017/jfm.2019.245

Valocchi, A. J., Bolster, D., & Werth, C. J. (2019). Mixing-limited reactions in porous media. *Transport in Porous Media*, *130*, 157–182. https://doi.org/10.1007/s11242-018-1204-1

Wallace, C. D., Sawyer, A. H., Soltanian, M. R., & Barnes, R. T. (2020). Nitrate removal within heterogeneous riparian aquifers under tidal influence. *Geophysical Research Letters*, *47*, e2019GL085699. https://doi.org/10.1029/2019GL085699

Werth, C. J., Cirpka, O. A., & Grathwohl, P. (2006). Enhanced mixing and reaction through flow focusing in heterogeneous porous media. *Water Resources Research*, *42*(12), W12414. https://doi.org/10.1029/2005WR004511

Wright, E., Richter, D. H., & Bolster, D. (2017). Effects of incomplete mixing on reactive transport in flows through heterogeneous porous media. *Physical Review Fluids*, *2*(11), 14501. https://doi.org/10.1103/PhysRevFluids.2.114501

Wu, J., Lester, D. R., Trefry, M. G., & Metcalfe, G. (2020a). When do complex transport dynamics arise in natural groundwater systems? *Water Resources Research*, *56*(2). e2019WR025982. https://doi.org/10.1029/2019WR025982

Wu, L., Gomez-Velez, J. D., Krause, S., Wörman, A., Singh, T., Nützmann, G., & Lewandowski, J. (2020b). How does daily groundwater table drawdown affect the diel rhythm of hyporheic exchange? *Hydrology and Earth System Sciences Discussions*, 1–25. https://doi.org/10.5194/hess-2020-288

Wu, L., Singh, T., Gomez-Velez, J., Nützmann, G., Wörman, A., Krause, S., & Lewandowski, J. (2018). Impact of dynamically changing discharge on hyporheic exchange processes under gaining and losing groundwater conditions. *Water Resources Research*, *54*(12), 10,076-10,093. https://doi.org/10.1029/2018WR023185

Ye, Y., Chiogna, G., Cirpka, O., Grathwohl, P., & Rolle, M. (2015a). Experimental investigation of compound-specific dilution of solute plumes in saturated porous media: 2-D vs. 3-D flow-through systems. *Journal of Contaminant Hydrology*, *172*, 33–47. https://doi.org/10.1016/j.jconhyd.2014.11.002

Ye, Y., Chiogna, G., Cirpka, O. A., Grathwohl, P., & Rolle, M. (2015b). Experimental evidence of helical flow in porous media. *Physical Review Letter*, *115*(19). 194502. https://doi.org/10.1103/PhysRevLett.115.194502

Ye, Y., Chiogna, G., Cirpka, O. A., Grathwohl, P., & Rolle, M. (2015c). Enhancement of plume dilution in two-dimensional and three-dimensional porous media by flow focusing in high-permeability inclusions. *Water Resources Research*, *51*, 5582–5602. https://doi.org/10.1002/2015WR016962

Ye, Y., Chiogna, G., Lu, C., & Rolle, M. (2018). Effect of anisotropy structure on plume entropy and reactive mixing in helical flows. *Transport in Porous Media*, *121*, 315–332. https://doi.org/10.1007/s11242-017-0964-3

Zhang, C., Dehoff, K., Hess, N., Oostrom, M., Wietsma, T. W., Valocchi, A. J., et al. (2010). Pore-scale study of transverse mixing induced $CaCO_3$ precipitation and permeability reduction in a model subsurface sedimentary system. *Environmental & Science Technology*, *44*(20), 7833–7838. https://doi.org/10.1021/es1019788

Zhang, P., DeVries, S. L., Dathe, A., & Bagtzoglou, A. C. (2009). Enhanced mixing and plume containment in porous media under time-dependent oscillatory flow. *Environmental Science & Technology*, *43*(16), 6283–6288. https://doi.org/10.1021/es900854r

Ziliotto, F., Basilio Hazas, M., Rolle, M., & Chiogna, G. (2021). Mixing enhancement mechanisms in aquifers affected by hydropeaking: Insights from flow-through laboratory experiments. *Mendeley Data*. V2. https://doi.org/10.17632/sx9gj2mhhm.2

References From the Supporting Information

Arntzen, E. V., Geist, D. R., & Dresel, P. E. (2006). Effects of fluctuating river flow on groundwater/surface water mixing in the hyporheic zone of a regulated, large cobble bed river. *River Research and Applications*, *22*(8), 937–946. https://doi.org/10.1002/rra.947

Cruz, V., & Silva, O. (2001). Hydrogeologic framework of Pico Island, Azores, Portugal. *Hydrogeology Journal*, *9*(2), 177–189. https://doi.org/10.1007/s100400000106

Fakir, Y., & Razack, M. (2003). Hydrodynamic characterization of a Sahelian coastal aquifer using the ocean tide effect (Dridrate Aquifer, Morocco). *Hydrological Sciences Journal*, *48*(3), 441–454. https://doi.org/10.1623/hysj.48.3.441.45281

Fette, M. W. (2005). *Tracer studies of river-groundwater interaction under hydropeaking conditions (Doctoral Thesis)*: Swiss Federal Institute of Technology Zurich.

Maier, H. S., & Howard, K. W. F. (2011). Influence of oscillating flow on hyporheic zone development. *Ground Water*, *49*(6), 830–844. https://doi.org/10.1111/j.1745-6584.2010.00794.x

Sawyer, A. H., Cardenas, M. B., Bomar, A., & Mackey, M. (2009). Impact of dam operations on hyporheic exchange in the riparian zone of a regulated river. *Hydrological Processes*, *23*(15), 2129–2137. https://doi.org/10.1002/hyp.7324

Smith, A. J. (1999). *Application of a tidal method for estimating aquifer diffusivity: Swan river, Western Australia: CSIRO Land and water*. Report No. 13/99. Retrieved from http://hdl.handle.net/102.100.100/213098?index=1

Smith, A. J., & Hick, W. P. (2001). *Hydrogeology and aquifer tidal propagation in Cockburn Sound, Western Australia: CSIRO Land and water*. Technical Report 6/01. https://doi.org/10.4225/08/58791689a6f92

Townley, L. R. (1995). The response of aquifers to periodic forcing. *Advances in Water Resources*, *18*(3), 125–146. https://doi.org/10.1016/0309-1708(95)00008-7

Trefry, M. G., & Bekele, E. (2004). Structural characterization of an island aquifer via tidal methods. *Water Resources Research*, *40*(1). https://doi.org/10.1029/2003WR002003

Trefry, M. G., & Johnston, C. D. (1998). Pumping test analysis for a tidally forced aquifer. *Ground Water*, *36*(3), 427–433. https://doi.org/10.1111/j.1745-6584.1998.tb02813.x

van Genuchten, M. T., Leij, F. J., Skaggs, T. H., Toride, N., Bradford, S. A., & Pontedeiro, E. M. (2013). Exact analytical solutions for contaminant transport in rivers 1. The equilibrium advection-dispersion equation. *Journal of Hydrology and Hydromechanics*, *61*(2), 146–160. https://doi.org/10.2478/johh-2013-0020

Wu, J., Lester, D. R., Trefry, M. G., & Metcalfe, G. (2020). When do complex transport dynamics arise in natural groundwater systems? *Water Resources Research*, *56*(2). https://doi.org/10.1029/2019WR02598